



Research Article

Mathematical Modeling of Dog Rabies Transmission Dynamics Using Optimal Control Analysis

Demsis Dejene Hailemichael* , Geremew Kenassa Edessa, Purnachandra Rao Koya

Department of Mathematics, Wollega University, Nekemte, Ethiopia
Email: demsish@wollegauniversity.edu.et

Received: 16 January 2023; **Revised:** 6 May 2023; **Accepted:** 11 May 2023

Abstract: An ideal control method for the dynamics of dog rabies transmission is provided in this study. Given the nature of the disease and the fact that contact behavior varies, we divided the infected compartment into prodromal and furious compartments in the current updated model, which is an extension of the previous SEIR model. Vaccination and culling are two disease-controlling strategies used in the current model, and their effects are examined. It is possible to compute the basic reproduction number using the next-generation matrix. We study the stability, sensitivity analysis, endemic equilibrium, disease-free equilibrium, and stability of the optimal control model. According to the numerical simulation, which utilizes approximations for parameter values, the most efficient strategy to prevent the spread of rabies is a combination of vaccination and the culling of infected dogs. Using ode45 from MATLAB, this numerical simulation investigation was carried out. According to our research, the annual dog birth rate is a factor that influences the incidence of rabies. The state equations, adjoint equations, and the optimal condition that sets the controls by Pontryagin's Maximum/Minimum principle can all be used to construct the optimal control system. The body of the article contains the findings and discussions in an ordered manner.

Keywords: rabies, optimal control, vaccination, culling, sensitive index

MSC: 92-10, 49J15

1. Introduction

The majority of rabies infections in humans are carried by dogs worldwide [1]. All mammalian species and other animals are most commonly impacted by rabies, an acute and fatal zoonotic viral infection. Animal saliva is not the only fluid in which the rabies virus can be found; tears, urine, semen, and other fluids can also carry it [2]. The virus's death rate is certain once clinical symptoms start to show up because it attacks the central nervous system and causes neurological symptoms in the brain [3].

The WHO 2021 report [4] states that while the incubation period for rabies is normally 2-3 months, it can also range from 1 week to 1 year depending on the viral load and the location of the virus's entry. A fever, pain, and an unusual or unexplained tingling, prickling, or burning feeling (paresthesia) at the site of the lesion are among the early signs of rabies. Progressive and deadly inflammation of the brain and spinal cord develops as the virus spread to the central nervous system. The disease comes in two different forms: Hyperactivity, excitable behavior, hydrophobia, and

even aerophobia are symptoms of rabid rabies. Cardio-respiratory arrest causes death a few days later. About 20% of all human cases of rabies result in paralysis. Compared to the furious form of rabies, this one has a less dramatic and typically longer course. Muscles begin to progressively paralysis at the bite or scratch location. Slowly, a coma sets in, and then there is death.

Vaccination and proper animal care have reduced the probability of dog rabies in various parts of the world. High-risk individuals, such as those who work with dogs or spend a lot of time in areas where rabies is prevalent, can get the required vaccines before being exposed. The disease can be prevented by rabies vaccinations and antibodies if treatment is given before the appearance of symptoms. By washing the exposed location with soap and water, iodine, povidone, or detergent for 15 minutes, the spread of the pathogens may be somewhat prevented [5].

In early models of rabies dynamics, the populations were divided into four categories: susceptible (S), exposed (E), infectious (I), and removed (R) [6]. A system of ordinary differential equations (ODEs) was used to explain the dynamics of rabies representing either single populations or linked meeting populations, from which a kind of pre-prediction regarding temporal and spatial patterns could be made. The basic SEIR compartmental framework was used to extract several critical elements of disease development and transmission in the early model of rabies. The model equation was used to calculate the virus's basic reproduction rate as well as the critical threshold point for the start of an epidemic.

The susceptible-exposed-infectious (SEI) model for the transmission of rabies was used to characterize areas around lakes, mountains, and significant rivers in a research conducted by [7] with the addition of the word "diffusion." In this investigation, the researchers found that infected animals can be quickly identified and eliminated even in areas with a high human population density and an environment similar to this one. Additionally, due to enhanced monitoring, researchers have hypothesized that reducing the rate of infection in these areas may help prevent the spread of rabies.

A susceptible-exposed-infectious-vaccinated (SEIV) model for the dog-human transmission of rabies was suggested by [8], taking into account both domestic and stray dogs. The results of their study showed that cases of rabies in China's Guangdong province would slowly decrease in the next few years and rise slightly thereafter, indicating that rabies cannot be managed or eradicated by using the method of culling that is frequently used. Based on the findings of their study, the authors suggested that rabies management and preventive strategies should include public education and rabies awareness, an increase in domestic dog vaccination rates, and a decrease in the number of stray dogs.

An ordinary differential equation can be used to represent the dynamics of population density or abundance. The initial group of organisms can be classified into four classes if the population is exposed to a viral infection: susceptible, exposed, infected, and possibly a recovered class. A potential objective is to select a control function that minimizes the spread of the infection and maximizes the number of the unaffected population given a diseased population and a control function that affects its dynamics. Optimal control theory may be used to theoretically solve a minimization problem of this type. This procedure is an analytical method applied to a given objective function that yields the optimal path to be taken by variables of a dynamic process in continuous time. In the disease models to be considered here, the dynamical process is represented by a system of ordinary differential equations (ODEs), and the objective function to minimize could depend upon some combination of the infected class and some control quantity. L.S. Pontryagin and his co-workers developed this method in the 1950s based on their formulation of the maximum principle for optimal control of ordinary differential equations [9]. In optimal control, variables are classified as state or control variables. The path of a state variable is determined by a first-order ordinary differential equation.

All the above studies have developed an SEIR-type mathematical model that can be used to determine and predict the spread of rabies diseases. So, in the SEIR models of dog rabies, it has been considered that the deaths are related to the disease. This fact is generalized and included all infected compartments. But in the present study considering the nature of the disease we divided the infected compartment into two compartments viz., prodromal and furious compartments since contact behavior is different. Further, it is assumed that deaths do not occur due to rabies in the prodromal stage but only in the furious stage. This is, therefore we are motivated to undertake this study to fulfilling this gap.

2. Methods

2.1 Model formulation

The modified SEI_pI_fR model is an extension of the existing SEIR model, which is used to describe the dynamics of dog rabies and to determine the amount of susceptible, exposed, infected, and recovered dogs in the population groups due to vaccinated dogs. During the disease, rabid animals exhibit three distinct behaviors [10]. Following infection, the dogs begin the prodromal phase, which is marked by shyness and isolation. They then begin the second phase, known as the furious phase, in which they become extremely aggressive. Finally, they enter the paralytic stage, after which they die. The infected population is separated into two groups based on their contact behavior: prodromal and furious dogs. The paralytic stage is assumed out since dogs who are paralyzed are unlikely to bite anyone. For the model, we divide the entire dog population into susceptible, exposed, infected within the prodromal stage, infected within the furious stage, and recover groups. Susceptible groups do not have the disease, but they are at risk of catching it if they come into contact with rabid dogs. Exposed individuals are those who have been exposed to the virus through bites or scratches but have yet to display symptoms. Individuals infected with rabies have clinical symptoms and are unlikely to recover because of the disease's nature. The recovered classes are those who were vaccinated and recovered before becoming contagious, whereas the rest were infected and died.

Table 1. Model Variables and their Description

Symbol	Description of the variables
S	Susceptible dog population at times t
E	Exposed dog population at the time t
I _p	Infectious dog population in the prodromal phase at time t
I _f	Infectious dog population with the furious phase at time t
R	Recovered dog population at the time t

Table 2. Model parameters and their description

Symbol	Description of the variables
A	The annual birth of the dog population
β	The rate of infectious dogs infecting the susceptible dog
δ	The incubation period of dog populations
ρ	Rate of prodromal to furious stage
θ	Vaccination rate of Susceptible dog populations
ε	The death rate due to rabies
μ	Natural death rate
α	The loss rate of vaccination immunity

The following are the model's assumptions: The way a dog can leave the susceptible group is to become recovery class at the rate of θ due to pre expose vaccination and exposed class at the transmission rate of β , the loss rate of the recovered class go to the susceptible class directly at the rate of α , the way a dog can leave the exposed group is to infected with prodromal I_p stage with the rate of δ , the way the dog can leave from the infected with prodromal I_p stage group to infected with furious I_f stage class is with the rate of ρ , the rate ε of the infected with furious I_f stage goes to death due to rabies, there is no chance to recover from the disease for all infected dogs, and the model parameters and state variables are all positive. Table 1 and Table 2 above, respectively, contain descriptions of the model's variables and parameters.

2.1.1 Model compartment and dynamics

The following ordinary differential equation represents the infection paths based on the transmission flowchart in Figure 1.

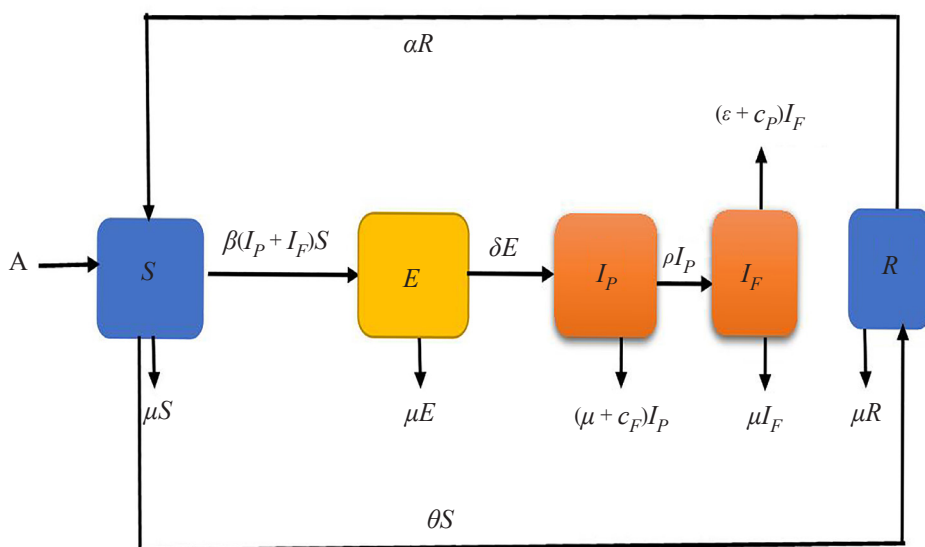


Figure 1. Flow diagram of the model

$$\left. \begin{aligned}
 \frac{dS}{dt} &= A - \beta(I_p + I_f)S - (\theta + \mu)S + \alpha R \\
 \frac{dE}{dt} &= \beta(I_p + I_f)S - (\delta + \mu)E \\
 \frac{dI_p}{dt} &= \delta E - (\rho + c_p + \mu)I_p \\
 \frac{dI_f}{dt} &= \rho I_p - (\varepsilon + c_f + \mu)I_f \\
 \frac{dR}{dt} &= \theta S - (\alpha + \mu)R
 \end{aligned} \right\} \quad (1)$$

$N(t)$ has a total population of:

$$N(t) = S(t) + E(t) + I_p(t) + I_f(t) + R(t)$$

2.2 Invariant region of the model

The overall number of dogs must be constrained in this situation. This means that the model system is evaluated inside the feasible zone for all $t \geq 0$ and that state variables and parameters are assumed to be positive. Take a look at the lemma below.

Lemma 1. The solution set $\{S(t), E(t), I_p(t), I_F(t), R(t)\} \in R_+^5$ of model system (1) is contained in the feasible region Ω .

Proof. The entire population of dogs changes over time due to the rise of individuals into the susceptible class. The following formula is used to calculate the rate of change in the overall dog population: $\frac{dN}{dt} = \frac{dS}{dt} + \frac{dE}{dt} + \frac{dI_p}{dt} + \frac{dI_F}{dt} + \frac{dR}{dt}$

$$\frac{dN}{dt} = A - \mu N - (\varepsilon + c_F)I_F - c_P I_P \quad (2)$$

Considering no disease-related mortality rate or culling impact, (2) becomes

$$\frac{dN}{dt} = A - \mu N \quad (3)$$

Assume, $\frac{dN}{dt} \leq 0$, $N = \frac{A}{\mu}$ and use the theorem in [11] to get: $0 \leq N \leq \frac{A}{\mu}$. As a result, (3) yields.

$$\frac{dN}{dt} \leq A - \mu N \quad (4)$$

After a few arithmetical checks, solve (4), and the potential solution for the dog population in the model system (1) is located within the region.

$$\Omega = \left\{ (S(t), E(t), I_p(t), I_F(t), R(t)) \in R_+^5, N \leq \frac{A}{\mu} \right\} \quad (5)$$

In this way, feasible solutions are contained. The common comparison theorem in [12] was used to determine the differential-difference.

$$N(t) \leq N(0)e^{-(\mu)t} + \frac{A}{\mu} (1 - e^{-(\mu)t}) \quad (6)$$

This leads to an estimate of $N(t) \rightarrow \frac{A}{\mu}$ as $t \rightarrow \infty$. This means that the infected state (E, I_p, I_F) of the population trend to zero as time goes to infinity. As a result, region Ω is pulling (attracting) all the solution in R_+^5 . Hence, the model system (1) is mathematically well-posed, biologically and epidemiologically correct.

2.3 Disease-Free Equilibrium Points (DFE)

The equation system (1) $\varepsilon_0 = (S^0, E^0, I_p^0, I_F^0, R^0)$. Denotes the model's disease-free equilibrium point. The steady-state results of a mathematical model that reflect the absence of disease are referred to as "disease-free equilibrium points." The exposed and infected with prodromal and furious compartments are where the unhealthy dog population is exclusively found, according to the compartmental classification of the dog population. As a result, the disease-free

equilibrium point ε_0 will be determined by setting $\frac{dS}{dt} = \frac{dR}{dt} = 0$ in a model system (1). In the absence of infection, $E^0 = I_p^0 = I_f^0 = 0$, and the disease-free equilibrium point ε_0 will then be calculated as

$$\varepsilon_0 = \left(\frac{A(\alpha + \mu)}{\mu(\theta + \alpha + \mu)}, 0, 0, 0, \frac{A\theta}{\mu(\theta + \alpha + \mu)} \right) \quad (7)$$

2.4 The effective reproduction number, R_e

In epidemiology, the basic reproduction number (or ratio) is a crucial concept. The number R_0 , abbreviated, measures how many secondary infections a primary infection could cause in a susceptible population. The key principle is that we now need to average the estimated number of new infections among all infected types. The next-generation matrix is defined as the square matrix G , where the i, j^{th} element, g_{ij} , indicates the expected number of type i . secondary infections created by a single infected individual of type j , assuming that the type i . population is fully susceptible [13]. That is, each member of the matrix G is a reproduction number with information on who infects whom. Once we get G , we'll be one step closer to R_0 .

The spectral radius of matrix G determines the basic reproduction number. The matrix G 's dominant eigenvalue is known as the spectral radius. Many attractive mathematical characteristics define the next-generation matrix [14]. Since the matrix is non-negative, there will always be a single, unique eigenvalue that is strictly greater than the others and is positive, real, and unique. Consider the G matrix for the next generation. It is divided into two sections: F and V^{-1} , where

$$F = \left[\frac{\partial F_i(\varepsilon_0)}{\partial X_j} \right] \text{ and } V = \left[\frac{\partial V_i(\varepsilon_0)}{\partial X_j} \right] \quad (8)$$

The F_i are the new infections, while the V_i transfer infections from one compartment to another. ε_0 is the disease-free equilibrium state. R_0 is the dominant eigenvalue of the matrix $G = FV^{-1}$.

We calculated our model of the effective reproduction number using the next-generation approach and the infected compartments from the system (1)

$$\left. \begin{aligned} \frac{dE}{dt} &= \beta(I_P + I_F)S - (\delta + \mu)E \\ \frac{dI_P}{dt} &= \delta E - (\rho + c_P + \mu)I_P \\ \frac{dI_F}{dt} &= \rho I_P - (\varepsilon + c_F + \mu)I_F \end{aligned} \right\} \quad (9)$$

$$F_i = \begin{bmatrix} \beta(I_P + I_F)S \\ 0 \\ 0 \end{bmatrix}, \quad F = \begin{bmatrix} 0 & \frac{A\beta(\alpha + \mu)}{\mu(\theta + \alpha + \mu)} & \frac{A\beta(\alpha + \mu)}{\mu(\theta + \alpha + \mu)} \\ 0 & 0 & 0 \\ 0 & 0 & 0 \end{bmatrix},$$

$$V_i = \begin{bmatrix} (\delta + \mu)E \\ (\rho + C_P + \mu)I_P - \delta E \\ (\varepsilon + C_F + \mu)I_F - \rho I_P \end{bmatrix}, \quad V = \begin{bmatrix} (\delta + \mu) & 0 & 0 \\ -\delta & (\rho + C_P + \mu) & 0 \\ 0 & -\rho & (\varepsilon + C_F + \mu) \end{bmatrix},$$

$$V^{-1} = \begin{pmatrix} \frac{1}{(\delta + \mu)} & 0 & 0 \\ \frac{1}{(\delta + \mu)(\rho + C_P + \mu)} & \frac{1}{(\rho + C_P + \mu)} & 0 \\ \frac{1}{(\delta + \mu)(\rho + C_P + \mu)(\varepsilon + C_F + \mu)} & \frac{\rho}{(\rho + C_P + \mu)(\varepsilon + C_F + \mu)} & \frac{1}{(\varepsilon + C_F + \mu)} \end{pmatrix},$$

$$\text{Eigenvalues}(FV^{-1}) = \begin{bmatrix} 0 \\ 0 \\ \frac{A\beta\delta(\varepsilon + C_P + \mu + \rho)}{\mu(\theta + \alpha + \mu)(\delta + \mu)(\rho + C_P + \mu)(\varepsilon + C_F + \mu)} \end{bmatrix}$$

As a result, the effective number is calculated as

$$R_e = \text{Spectral Radius}(FV^{-1}) = \frac{A\beta\delta(\varepsilon + C_P + \mu + \rho)}{\mu(\theta + \alpha + \mu)(\delta + \mu)(\rho + C_P + \mu)(\varepsilon + C_F + \mu)} \quad (10)$$

2.5 Endemic equilibrium points (ε_*)

Endemic equilibrium points are steady-state conditions in which the disease continues to impact the population. The endemic equilibrium point ε_* of the model is given by: $\varepsilon_* = (S^*, E^*, I_P^*, I_F^*, R^*)$ We set $\frac{dS}{dt} = \frac{dE}{dt} = \frac{dI_P}{dt} = \frac{dI_F}{dt} = \frac{dR}{dt} = 0$ at the system (1) and Solve for S, E, I_P, I_F, R we get:

$$S^* = \frac{(\delta + \mu)(\rho + C_P + \mu)(\varepsilon + C_F + \mu)}{\beta\delta(\varepsilon + C_P + \mu + \rho)} = \frac{A(\varepsilon + C_P + \mu + \rho)}{\mu(\theta + \alpha + \mu)R_e}, \text{ since } R_e = \frac{A\beta\delta(\varepsilon + C_P + \mu + \rho)}{\mu(\theta + \alpha + \mu)(\delta + \mu)(\rho + C_P + \mu)(\varepsilon + C_F + \mu)}$$

$$E^* = \frac{A}{(\delta + \mu)} \left[1 - \frac{1}{(\alpha + \mu)R_e} \right]$$

$$I_P^* = \frac{A\delta}{(\delta + \mu)(\rho + C_P + \mu)} \left[1 - \frac{1}{(\alpha + \mu)R_e} \right]$$

$$I_F^* = \frac{A\delta\rho}{(\varepsilon + C_F + \mu)(\delta + \mu)(\rho + C_P + \mu)} \left[1 - \frac{1}{(\alpha + \mu)R_e} \right]$$

$$R^* = \frac{A\theta}{\mu(\theta + \alpha + \mu)(\alpha + \mu)R_e} \quad (11)$$

3. Stability analysis

3.1 Local stability of the disease-free equilibrium point

The Jacobian matrix of Model System (1) at $\varepsilon_0 = (S^0, E^0, I_P^0, I_F^0, R^0) = \left(\frac{A(\alpha + \mu)}{\mu(\theta + \alpha + \mu)}, 0, 0, 0, \frac{A\theta}{\mu(\theta + \alpha + \mu)} \right)$ is evaluated to investigate local stability at the disease-free equilibrium point (DEF).

Theorem. If $R_0 < 1$ then disease-free equilibrium point ε_0 is locally asymptotic stable, and if $R_0 \geq 1$, ε_0 is unstable.

For the model system, we derive Jacobin matrices (1). This is accomplished by differentiating the system's equation in terms of the state variables S, E, I_p, I_F and R . Let J_{ε_0} be the Jacobian matrix evaluating at the disease-free equilibrium ε_0

$$J_{\varepsilon_0} = \begin{bmatrix} -\beta(I_P^0 + I_F^0) - (\theta + \mu) & 0 & -\beta S^0 & -\beta S^0 & \alpha \\ \beta(I_P^0 + I_F^0) & -(\delta + \mu) & \beta S^0 & \beta S^0 & 0 \\ 0 & \delta & -(\rho + c_p + \mu) & 0 & 0 \\ 0 & 0 & \rho & -(\varepsilon + c_F + \mu) & 0 \\ \theta & 0 & 0 & 0 & -(\alpha + \mu) \end{bmatrix} \quad (12)$$

The matrix in (12) is evaluated at the disease-free equilibrium point $(S^0, E^0, I_P^0, I_F^0, R^0) = \left(\frac{A(\alpha + \mu)}{\mu(\theta + \alpha + \mu)}, 0, 0, 0, \frac{A\theta}{\mu(\theta + \alpha + \mu)} \right)$ and the result is:

$$J_{\varepsilon_0} = \begin{bmatrix} -(\theta + \mu) & 0 & \frac{-\beta A(\alpha + \mu)}{\mu(\theta + \alpha + \mu)} & \frac{-\beta A(\alpha + \mu)}{\mu(\theta + \alpha + \mu)} & \alpha \\ 0 & -(\delta + \mu) & \frac{\beta A(\alpha + \mu)}{\mu(\theta + \alpha + \mu)} & \frac{\beta A(\alpha + \mu)}{\mu(\theta + \alpha + \mu)} & 0 \\ 0 & \delta & -(\rho + c_p + \mu) & 0 & 0 \\ 0 & 0 & \rho & -(\varepsilon + c_F + \mu) & 0 \\ \theta & 0 & 0 & 0 & -(\alpha + \mu) \end{bmatrix} \quad (13)$$

Let, $a_1 = (\theta + \mu)$, $a_2 = -(\delta + \mu)$, $a_3 = (\rho + c_p + \mu)$, $a_4 = (\varepsilon + c_F + \mu)$, $a_5 = (\alpha + \mu)$, $a_6 = \frac{\beta A(\alpha + \mu)}{\mu(\theta + \alpha + \mu)}$, substituting these in Matrix (13) yield's

$$\begin{bmatrix} -a_1 & 0 & -a_6 & -a_6 & \alpha \\ 0 & -a_2 & a_6 & a_6 & 0 \\ 0 & \delta & -a_3 & 0 & 0 \\ 0 & 0 & \rho & -a_4 & 0 \\ \theta & 0 & 0 & 0 & -a_5 \end{bmatrix} \quad (14)$$

$|J_{\varepsilon_0} - \lambda I| = 0$ is the characteristic equation of the matrix J_{ε_0} . I represent a class 5×5 identity matrix in this instance, and λ is the eigenvalue. With the help of this characteristic equation, we talk about the sign of Eigenvalues.

$$|J_{\varepsilon_0} - \lambda I| = \begin{vmatrix} -(a_1 + \lambda) & 0 & -a_6 & -a_6 & \alpha \\ 0 & -(a_2 + \lambda) & a_6 & a_6 & 0 \\ 0 & \delta & -(a_3 + \lambda) & 0 & 0 \\ 0 & 0 & \rho & -(a_4 + \lambda) & 0 \\ \theta & 0 & 0 & 0 & -(a_5 + \lambda) \end{vmatrix} = 0$$

$$-(a_1 - \lambda) \begin{vmatrix} -(a_2 + \lambda) & a_6 & a_6 & 0 \\ \delta & -(a_3 + \lambda) & 0 & 0 \\ 0 & \rho & -(a_4 + \lambda) & 0 \\ 0 & 0 & 0 & -(a_5 + \lambda) \end{vmatrix} + \theta \begin{vmatrix} 0 & -a_6 & -a_6 & \alpha \\ -(a_2 + \lambda) & a_6 & a_6 & 0 \\ \delta & -(a_3 + \lambda) & 0 & 0 \\ 0 & \rho & -(a_4 + \lambda) & 0 \end{vmatrix} = 0$$

$$(a_1 - \lambda)(a_5 - \lambda) \begin{vmatrix} -(a_2 + \lambda) & a_6 & a_6 \\ \delta & -(a_3 + \lambda) & 0 \\ 0 & \rho & -(a_4 + \lambda) \end{vmatrix} - \theta \alpha \begin{vmatrix} -(a_2 + \lambda) & a_6 & a_6 \\ \delta & -(a_3 + \lambda) & 0 \\ 0 & \rho & -(a_4 + \lambda) \end{vmatrix} = 0$$

$$[(a_1 - \lambda)(a_5 - \lambda) - \theta \alpha] \begin{vmatrix} -(a_2 + \lambda) & a_6 & a_6 \\ \delta & -(a_3 + \lambda) & 0 \\ 0 & \rho & -(a_4 + \lambda) \end{vmatrix} = 0$$

$$(a_1 - \lambda)(a_5 - \lambda) - \theta \alpha = 0 \quad (15)$$

Or

$$\begin{vmatrix} -(a_2 + \lambda) & a_6 & a_6 \\ \delta & -(a_3 + \lambda) & 0 \\ 0 & \rho & -(a_4 + \lambda) \end{vmatrix} = 0 \quad (16)$$

From Equation (15), we obtain two eigenvalues. $(\theta + \mu + \lambda)(\alpha + \mu + \lambda) - \theta \alpha = 0$, since $a_1 = (\theta + \mu)$ and $a_5 = (\alpha + \mu)$. We arrive after some computations

$$\lambda^2 + (\theta + \alpha + 2\mu)\lambda + \mu(\theta + \alpha + \mu) = 0$$

The quadratic equation demands that both eigenvalues be real and negative and that we also satisfy the other

requirements.

$$\lambda_{1,2} = -(\theta + \alpha + 2\mu) \frac{\pm \sqrt{(\theta + \alpha + 2\mu)^2 - 4(1)\mu(\theta + \alpha + 2\mu)}}{2(1)} < 0$$

$$\sqrt{(\theta + \alpha + 2\mu)^2 - 4(1)\mu(\theta + \alpha + 2\mu)} < (\theta + \alpha + 2\mu)^2$$

Squaring both sides we get $(\theta + \alpha + 2\mu)^2 - 4(1)\mu(\theta + \alpha + 2\mu) < (\theta + \alpha + 2\mu)^2$.

This implies that $-4(1)\mu(\theta + \alpha + \mu) < 0$ the parameter's values θ, α, μ are positive. We can conclude from the justification given above that the eigenvalues λ_1 and λ_2 are distinct and negative. Three eigenvalues are obtained from Equation (16).

$$\begin{vmatrix} -(a_2 + \lambda) & a_6 & a_6 \\ \delta & -(a_3 + \lambda) & 0 \\ 0 & \rho & -(a_4 + \lambda) \end{vmatrix} = 0$$

This implies

$$\begin{vmatrix} (a_2 + \lambda) & -a_6 & -a_6 \\ \delta & (a_3 + \lambda) & 0 \\ 0 & -\rho & (a_4 + \lambda) \end{vmatrix} = 0$$

$$(a_2 + \lambda) \begin{vmatrix} (a_3 + \lambda) & 0 \\ -\rho & (a_4 + \lambda) \end{vmatrix} + \delta \begin{vmatrix} -a_6 & -a_6 \\ -\rho & (a_4 + \lambda) \end{vmatrix} = 0$$

$$(a_2 + \lambda)(a_3 + \lambda)(a_4 + \lambda) - \delta a_6(a_4 + \lambda) - \rho a_6 = 0 \tag{17}$$

It took some organizing to arrive at the equation (17).

$$\lambda^3 + (a_2 + a_3 + a_4)\lambda^2 + (a_2a_3 + a_2a_4 + a_3a_4 - \delta a_6)\lambda + (1 - R_0) = 0$$

The characteristic polynomial follows

$$P(\lambda) = \lambda^3 + (a_2 + a_3 + a_4)\lambda^2 + (a_2a_3 + a_2a_4 + a_3a_4 - \delta a_6)\lambda + (1 - R_0) \tag{18}$$

3.1.1 Routh hurwitz stability criteria

The Routh Array, an array of the coefficients of the characteristic equation, serves as the foundation for Hurwitz and Routh's stability criterion. According to the Routh stability criteria, a system is considered stable if every term in the first column of the Routh Array created by its characteristic equation is positive if an $a_0 > 0$. If this criterion is not met, the system is considered unstable.

$$\begin{array}{l|l}
\lambda^3 & 1 \qquad (a_2a_3 + a_2a_4 + a_3a_4 - \delta a_6) \\
\lambda^2 & (a_2 + a_3 + a_4) \quad (1 - R_0) \\
\lambda & b_1 = \frac{(a_2 + a_3 + a_4)(a_2a_3 + a_2a_4 + a_3a_4 - \delta a_6)\lambda + (1 - R_0)}{(a_2 + a_3 + a_4)} \\
\lambda^0 & (1 - R_0)
\end{array}$$

According to the Routh-Hurwitz criteria, the three roots are distinct and negative if $b_1 > 0$ and $R_0 < 1$. Equation (18) shows that all eigenvalues are negative. To demonstrate the theorem, the system (1) must be locally asymptotically stable at the disease-free equilibrium point if $R_0 < 1$, otherwise it is unstable.

3.2 Global stability of disease-free equilibrium points

The study of local stability focuses on the smaller-scale changes that can affect a system's equilibrium. Only under conditions where the system is placed close to the equilibrium for local stability can the equilibrium be restored. Conversely, global stability describes what happens to a system's equilibrium on a large scale when the initial conditions for the model variables are not limited.

In the case of global stability, the equilibrium is always maintained, and the model's solutions approach the equilibrium for any beginning conditions. While local stability analysis of a system limits the analysis to a narrow region near the equilibrium point, global stability analysis of a system would permit the analysis to be broadened further than this restricted region. Using the technique described by [15], we analyze the system's (1) DFE points' overall stability in this instance. The following is the structure of our model in system 1.

$$\left. \begin{array}{l} \frac{dx}{dt} = B_0(x - x_{\varepsilon_0}) + B_1y \\ \frac{dy}{dt} = B_2y \end{array} \right\} \quad (19)$$

Whereas $x \in \mathfrak{R}_+^5$, represents various exposed and infected individuals, represents various classes of susceptible and immunized individuals. The notation $x(\varepsilon_0)$ denotes a vector of length equal to x at DFE point ε_0 . We define the following concerning the system (1):

$$x = \begin{bmatrix} S \\ R \end{bmatrix}, y = \begin{bmatrix} E \\ I_P \\ I_F \end{bmatrix} \text{ and } x_{\varepsilon_0} = \begin{bmatrix} \frac{A(\alpha + \mu)}{\mu(\theta + \alpha + \mu)} \\ A\theta \\ \frac{A\theta}{\mu(\theta + \alpha + \mu)} \end{bmatrix}, x - x_{\varepsilon_0} = \begin{bmatrix} S - \frac{A(\alpha + \mu)}{\mu(\theta + \alpha + \mu)} \\ R - \frac{A\theta}{\mu(\theta + \alpha + \mu)} \end{bmatrix}$$

The global stability of the disease-free equilibrium requires that we demonstrate:

- i. B_0 should be a matrix whose eigenvalues are real and negative; and
- ii. B_2 should be a Metzler matrix.

Using system (1) and the representation shown in (19), the two equations can be rewritten as follows:

- i. B_0 should be a matrix whose eigenvalues are real and negative; and

$$\begin{bmatrix} A - \beta(I_P + I_F)S - (\theta + \mu)S + \alpha R \\ \theta S - (\alpha + \mu)R \end{bmatrix} = B_0 \begin{bmatrix} S - \frac{A(\alpha + \mu)}{\mu(\theta + \alpha + \mu)} \\ R - \frac{A\theta}{\mu(\theta + \alpha + \mu)} \end{bmatrix} + B_1 \begin{bmatrix} I_P \\ I_F \end{bmatrix}$$

$$\begin{bmatrix} A - (\theta + \mu)S + \alpha R \\ -(\alpha + \mu)R \end{bmatrix} + \begin{bmatrix} -\beta(I_P + I_F)S \\ \theta S \end{bmatrix} = B_0 \begin{bmatrix} S - \frac{A(\alpha + \mu)}{\mu(\theta + \alpha + \mu)} \\ R - \frac{A\theta}{\mu(\theta + \alpha + \mu)} \end{bmatrix} + B_1 \begin{bmatrix} I_P \\ I_F \end{bmatrix}$$

B_0, B_1 is the jacobian of the left sides given by

$$B_0 = \begin{bmatrix} -(\theta + \mu) & \alpha \\ 0 & -(\alpha + \mu) \end{bmatrix} \text{ and } B_1 = \begin{bmatrix} -\beta S^* & -\beta S^* \\ 0 & 0 \end{bmatrix}$$

ii. B_2 should be a Metzler matrix.

$$\begin{bmatrix} \beta(I_P + I_F)S - (\delta + \mu)E \\ \delta E - (\rho + c_P + \mu)I_P \\ \rho I_P - (\varepsilon + c_F + \mu)I_F \end{bmatrix} = B_2 = \begin{bmatrix} E \\ I_P \\ I_F \end{bmatrix}$$

B_2 is the left-side jacobian provided by

$$B_2 = \begin{bmatrix} -(\delta + \mu) & \frac{A\beta(\alpha + \mu)}{\mu(\theta + \alpha + \mu)} & \frac{A\beta(\alpha + \mu)}{\mu(\theta + \alpha + \mu)} \\ \delta & -(\rho + C_P + \mu) & 0 \\ 0 & \rho & -(\varepsilon + C_F + \mu) \end{bmatrix}$$

As a result, it is clear that matrix B_0 has real and negative eigenvalues in the principal diagonal and is an upper triangular matrix. The values of the eigenvalues are $-(\theta + \mu)$, and $-(\alpha + \mu)$. The fact that matrix B_2 includes non-negative off-diagonal elements and that all of its parameters are positive shows that it is a Metzler matrix. This shows that the disease-free equilibrium points of system (1) are globally asymptotically stable in the region. This leads to the critical theorem that follows.

Theorem. The disease-free equilibrium point is globally asymptotically stable in the region if $R_e < 1$ and unstable in the region Ω if $R_e > 1$.

4. Sensitivity analysis

Sensitivity analysis is a method for determining how “sensitive” a model is to changes through its structure and parameter values. By analyzing the uncertainties that are usually linked to model parameters, sensitivity analysis helps in improving model reliability [16]. Sensitivity indices enable us to evaluate the relative change in a state variable when

a parameter is changed. Sensitivity analysis is frequently used to evaluate the model predictions' stability to parameter values. As a result, we use it to determine which variables have a significant impact on R_e and ought to be addressed by intervention measures. If the result is negative, the relationship between the parameters and R_e is inversely proportional. On the other hand, a positive sensitivity index means that the parameter has a direct impact on R_e . The ratio of a variable's relative change to a parameter's relative change is known as the normalized forward sensitivity index. Additionally, the parameter values listed in Table 3 below are a focus of its research.

Table 3. Parameters and their values for model (1) (unit: year⁻¹).

Parameter	Value	Interpretation	Source
A	20,000	The annual birth of the dog population	[17]
β	1.29×10^{-5}	The rate of infectious dogs infecting the susceptible dog	[17]
δ	0.17	The incubation period of dog populations	[17]
ρ	0.821	Rate of propagation of furiousness among dogs	Assumed
θ	0.5	Vaccination rate of Susceptible dog populations	[17]
ε	1	The death rate due to rabies	[18]
μ	0.083	Natural death rate	[19]
C_P	0.5	Rabid dog culling rate (with prodromal stage)	Assumed
C_F	0.5	Rabid dog culling rate (with furious stage)	Assumed
α	1	The loss rate of vaccination immunity	[19]

If the variable is a differentiable function of the parameter, the following definition applies to the sensitivity index:

Definition. The following is the definition of the variable X 's parameter-dependent normalized forward sensitivity index:

$$S_{\omega}^X = \frac{\partial X}{\partial \omega} \times \frac{\omega}{X}$$

In our case, we have the effective reproduction number $R_e = \frac{A\beta\delta(\varepsilon + C_P + \mu + \rho)}{\mu(\theta + \alpha + \mu)(\delta + \mu)(\rho + C_P + \mu)(\varepsilon + C_F + \mu)}$.

The model yields the following as the sensitivity index of R_e concerning R_e concerning, $\delta, \rho, \theta, \varepsilon, \mu, \alpha$:

$$S_{\beta}^{R_e} = \frac{\partial R_e}{\partial \beta} \times \frac{\beta}{R_e} = +1$$

Similarly, the sensitivity index of R_e concerning, $\delta, \rho, \theta, \varepsilon, \mu, \alpha$ is given in Table 3 as follows

Table 4. Sensitivity Indices of R_e

Parameter	Sensitivity Index Value
A	+1
β	+1
μ	-1.457518442
θ	-0.4616805171
α	-0.6317119394
ϵ	-0.2157385617
C_P	-0.1481386673
C_F	-0.3158559697
δ	0.3280632411
ρ	-0.2432436917

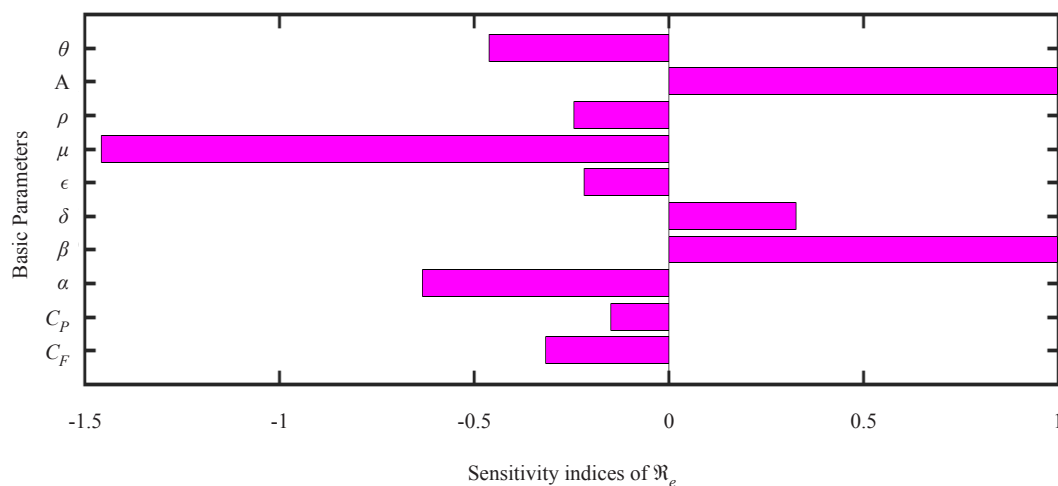


Figure 2. Sensitivity indices of the effective reproduction number

Table 4 and Figure 2 both demonstrate this. According to the sensitivity indices, the infection rate β , and annual births A are the most positive sensitive factors, which are then followed by the incubation duration δ . The effective reproduction number R_e will rise as these parameters are raised [20]. The natural mortality rate μ is also the parameter with the highest negative sensitivity, followed by the rate of immunity loss from vaccinations α , the rate of vaccination of susceptible dogs, Furious stage rabid dog culling rate C_F , rabies death rate ϵ , prodromal to furious stage rate ρ , and the prodromal stage rabid dog culling rate. As a result, the effective reproduction number R_e drops as these parameters are increased. Therefore, based on the sensitivity indices, the natural death rate μ , followed by the infection rate β and annual births A , is the most sensitive parameter.

5. Numerical simulations

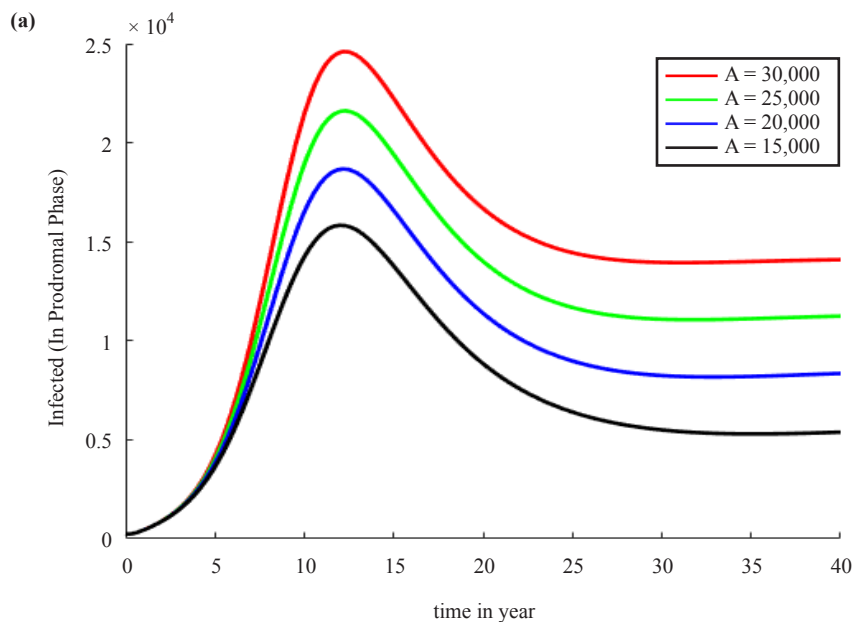
In this section, we provide numerical simulations to support the theoretical findings from the sections before. In our investigation, Figure 4 (a) and (b) show the test of various vaccination and culling rates and their impact on each group's curve. These graphs show various vaccination rates and how they affect the peak of the infection curve over time. The infected individuals' time-dependent curve demonstrates that when the percentage of individuals that have received vaccinations rises, the peak of the infected individuals' curve decreases [21].

The parameter values in Table 3, which are mostly obtained from published rabies research, are used to demonstrate our theoretical findings. Additionally, numerical analyses will be used to show how sensitive certain parameters are about the virus's endemic regions and control. Its research is also focused on the parameter values in Table 3 and the initial condition values shown in Table 5.

Table 5. Initial conditions used in the rabies model.

State Variable	S	E	I_P	I_F	R
The initial value is	300,000	8,000	150	250	50,000

According to the simulated curves in Figure 3 (a) and (b), a large number of dogs recruited into the susceptible dog's compartment will result in a large increase in the number of infected (in both the prodromal and furious phases), so reducing annual dog birth is critical to reducing rabies diseases. This demonstrates the importance of reducing dog rabies infection by focusing on the annual birth rate of the dog population.



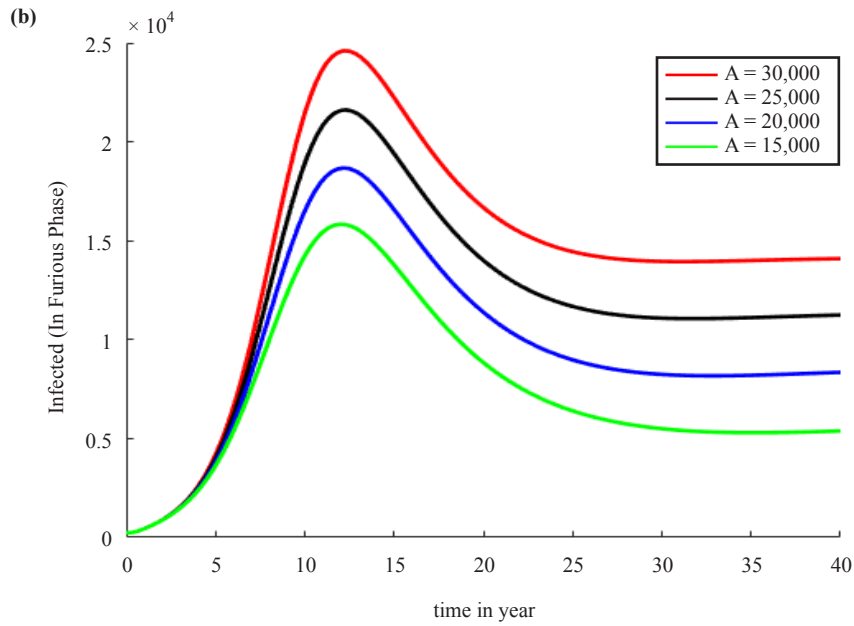
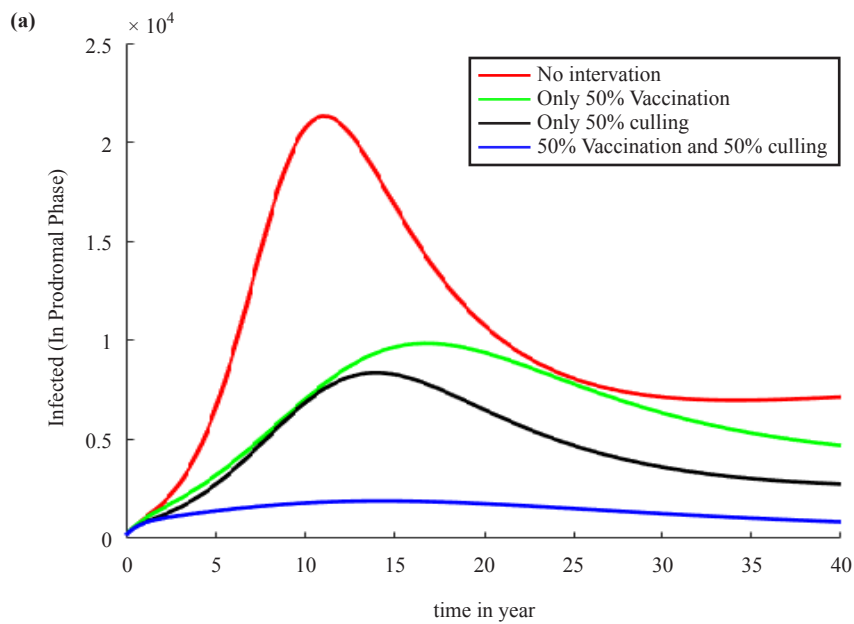


Figure 3. The effect of annual birth on the number of infected dog rabies, (a) Infected dog in the prodromal phase; (b) Infected dog in Furious phase

Figure 4 (a) and (b) show that intervention is very efficient in reducing the number of infected dogs in the prodromal and furious phases. When we compare curves for both infected in prodromal and furious phase dogs that had no intervention with those that received the intervention. When comparing the two interventions, it indicates that a combination of culling and vaccination has the greatest impact on reducing the number of infected dogs in the prodromal and furious phases, followed by culling alone and then vaccination alone. In both infected prodromal and furious phase group populations, culling alone is more effective than vaccination alone. To control the spread of rabies, it is, therefore, more effective to use both vaccine and culling intervention methods rather than individual intervention.



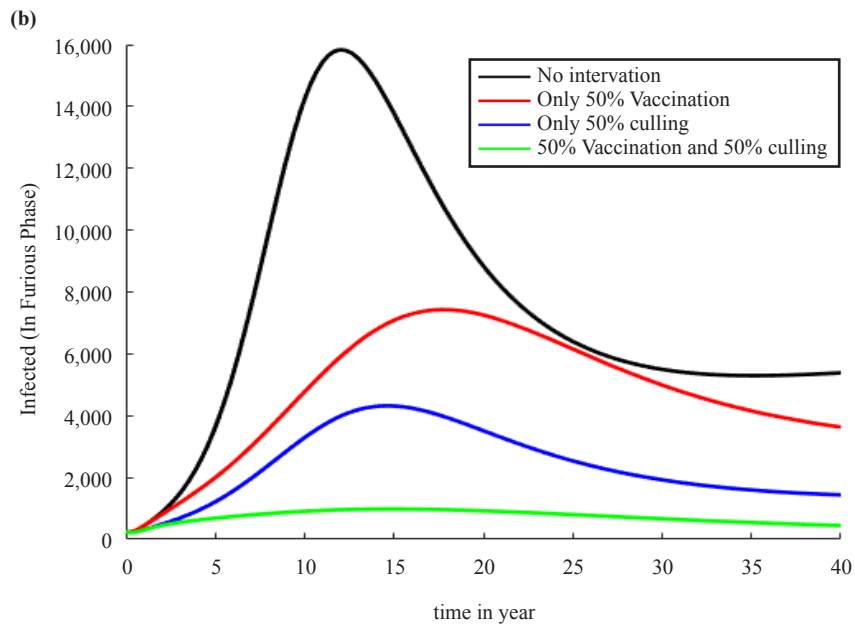
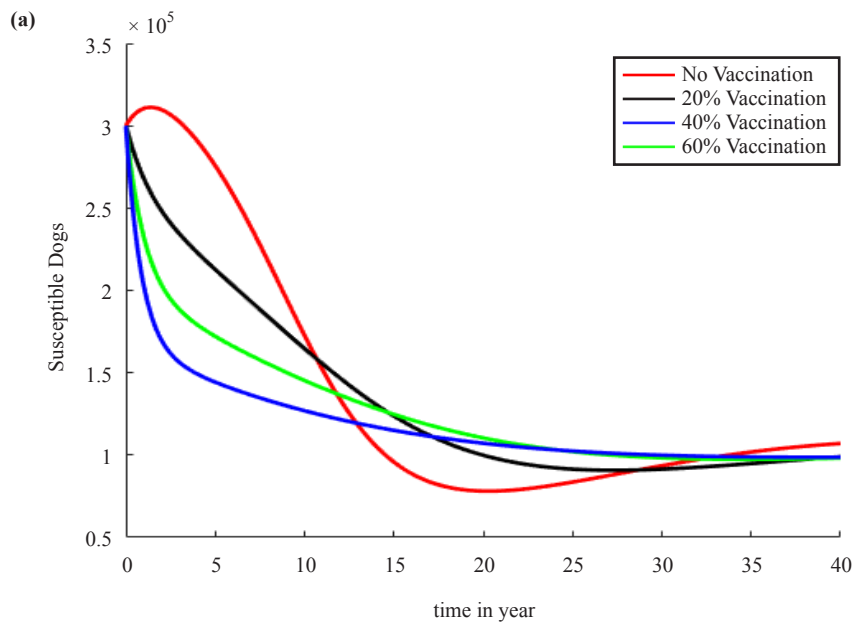


Figure 4. The effect of vaccination and culling on the Infected, (a) Infected dog in the prodromal phase; (b) Infected dog in Furious phase

Figure 5 (a) and (b) shows that a high vaccination rate for dogs results in an increase in recovered dogs and a decrease in susceptible dogs, respectively. This suggests that the vaccination of dogs is a successful method for reducing rabies in the dog population.



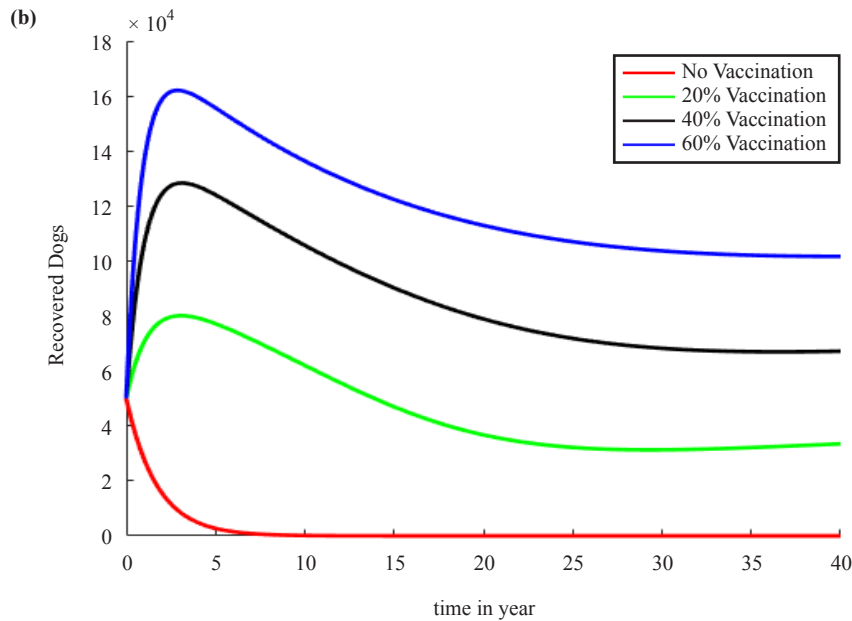


Figure 5. The effect of Vaccination rate θ on Susceptible and Recover class dogs, (a) Susceptible dogs; (b) Recovered dogs

6. Optimal control

We first concentrate on the optimal control of a single ODE because the models presented in this study are systems of five differential equations. The state is represented by $x(t)$, and the control is denoted by $u(t)$. The state function, $x(t)$, satisfies the ODE describing the state $x(t)$. The state of ODE is impacted by the control [22].

$$\frac{dx}{dt} = g(t, x(t), u(t)). \quad (20)$$

The aim, represented by the objective function, is affected by both $u(t)$ and $x(t)$ the objective function is usually expressed as an integral expression including the state and control variables. We want to identify an optimal control and state that maximizes (or minimizes) the value of our goal function. The optimal control problem can be expressed as follows:

$$\max_{u \in U} \int_0^T f(t, x(t), u(t)) dt \quad (21)$$

Subject to:

$$g(t, x(t), u(t)), \text{ where } x(0) = x_0 \text{ and } x(T) \text{ are free.} \quad (22)$$

We use the control set U of Lebesgue measurable functions. The optimal control, represented by $u^*(t)$, yields the maximum. Pontryagin's Maximum Principle [23] can be used to formulate the first-order necessary conditions in their most following components, assuming that f and g are continuously differentiable in their arguments.

Theorem. Pontryagin's Maximum Principle If $u^*(t)$ and $x^*(t)$ are optimal for the problem (20), (21), and (22) then there exists an adjoint variable $\lambda(t)$ such that

$$H(t; x^*(t), u(t), \lambda(t)) \leq H(t, x^*(t), u^*(t), \lambda(t)),$$

Where the Hamiltonian H is defined by at each moment

$$H(t; x(t), u(t), \lambda(t)) = f(t, x(t), u(t)) + \lambda(t)g(t, x(t), u(t)),$$

and

$$\frac{d\lambda}{dt} = -\frac{\partial H(t, x(t), u(t), \lambda(t))}{\partial x}, \lambda(t) = 0.$$

The adjoint variable's final time condition is the transversality condition. Using this idea, the problem of constructing a control that maximizes the objective function while taking into consideration the state ODE and initial condition was transformed into a problem of optimizing the Hamiltonian point-wise. As was already stated, the definition of the Hamiltonian is

$$H(t, x, u, \lambda) = f(t, x, u) + \lambda g(t, x, u) = (\text{Integrand}) + (\text{adjoint}) (\text{RHS of ODE}).$$

Maximizing H concerning u at u^* can be used to provide the requisite conditions. They are the necessary conditions can be created by the maximization of H about u at u^* . They are

$$\frac{\partial H}{\partial u} = 0 \Rightarrow \frac{\partial f}{\partial u} + \lambda \frac{\partial g}{\partial u} = 0 \text{ (Optimality equation),}$$

$$\lambda' = -\frac{\partial H}{\partial x} \Rightarrow \lambda' = -\left(\frac{\partial f}{\partial x} + \lambda \frac{\partial g}{\partial x}\right) \text{ (adjoint equation),}$$

and $\lambda(T) = 0$ (transversality condition). There is additional room for second-order conditions. Our potential is at its maximum. $\frac{\partial^2 H}{\partial u^2} \leq 0$ at $u = u^*$, and for minimization, we have $\frac{\partial^2 H}{\partial u^2} \leq 0$ at $u = u^*$. We started with two unknowns, u^* and x^* , and then added an adjoint variable, λ . Now we have three unknowns u^* , x^* , and λ . we can set $\frac{\partial H}{\partial u} \Big|_{u=u^*} = 0$ and solve for u^* . This characterization of the optimal control will be in terms of x^* and λ .

6.1 Objective functional

Assumed that $x(t) \in X \in \mathbb{R}^n$ is a state variable of model system (1) and $u(t) \in U \in \mathbb{R}^n$ are control variables at any time (t) with $(0) \leq t \leq T$, an optimum control problem involves determining a piecewise continuous control $u(t)$ and its corresponding state $x(t)$. Pontryagin's maximal principle [24] is used to optimize the cost functional $J[x(t), u(t)]$.

As a result, we proposed the following likelihood control strategies: The control effort aimed at improving the immunity of susceptible dogs is known as $u = \theta$ (preexposed prophylaxis). Our goal is to find optimal controls u^* that minimize the functional objective:

$$J = \min_{u \in U} \int_0^T \left[A_1 E + A_2 I_P + A_3 I_F + \frac{B}{2} u^2 \right] dt \quad (23)$$

Subject to:

$$\frac{dS}{dt} = A - \beta(I_P + I_F)S - (u + \mu)S + \alpha R$$

$$\frac{dE}{dt} = \beta(I_P + I_F)S - (\delta + \mu)E$$

$$\frac{dI_P}{dt} = \delta E - (\rho + c_P + \mu)I_P$$

$$\frac{dI_F}{dt} = \rho I_P - (\varepsilon + c_F + \mu)I_F$$

$$\frac{dR}{dt} = uS - (\alpha + \mu)R$$

$$S_0 > 0, E \geq 0, I_P \geq 0, I_F \geq 0, R \geq 0.$$

A_1 stands for the exposed class' weight constants, whereas A_1 and A_2 represent the prodromal and furious stages of the infected classes' weights, respectively. The weighting constant for the control is $B u^2$. Give an estimate of the rabies vaccine's cost. The degree of a vaccination's side effects is represented by the square of the control variables. The Hamiltonian equation is derived using the state variables $S = S^*$, $E = E^*$, $I_P = I_P^*$ and $R = R^*$ as Integrand + (adjoint) \times (RHS of the system (1)) using Pontryagin's maximum principle.

$$H = A_1 E^* + A_2 I_P^* + A_3 I_F^* + \frac{B_1}{2} u^2 + \lambda_1 \left[A - \beta(I_P^* + I_F^*)S^* - (u + \mu)S^* + \alpha R^* \right] + \lambda_2 \left[\beta(I_P^* + I_F^*)S^* - (\delta + \mu)E^* \right] \\ + \lambda_3 \left[\delta E^* - (\rho + c_P + \mu)I_P^* \right] + \lambda_4 \left[\rho I_P^* - (\varepsilon + c_F + \mu)I_F^* \right] + \lambda_5 \left[uS^* - (\alpha + \mu)R^* \right]$$

Consider the adjoint function's existence $\lambda_i, i = 1, 2, 3, 4, 5$ satisfying

$$\frac{d\lambda_1}{dt} = -\frac{\partial H}{\partial S^*} = \lambda_1 \left[\beta(I_P^* + I_F^*) + u + \mu \right] + \lambda_2 \beta(I_P^* + I_F^*) + \lambda_5 u,$$

$$\frac{d\lambda_2}{dt} = -\frac{\partial H}{\partial E^*} = \lambda_2 (\delta + \mu) - \lambda_3 \delta - A_1,$$

$$\frac{d\lambda_3}{dt} = -\frac{\partial H}{\partial I_P^*} = \lambda_1 \beta S^* + \lambda_3 (\rho + c_P + \mu) - A_2 - \lambda_2 \beta S^* - \lambda_4 I_P^*,$$

$$\frac{d\lambda_4}{dt} = -\frac{\partial H}{\partial I_F^*} = \lambda_1 \beta S^* + \lambda_4 (\varepsilon + c_F + \mu) - A_3 - \lambda_2 \beta S^*,$$

$$\frac{d\lambda_5}{dt} = -\frac{\partial H}{\partial R^*} = \lambda_5(\alpha + \mu) - \lambda_1\alpha. \quad (24)$$

With transversality condition $\lambda_i(T) = 0$ for $i = 1, 2, 3, 4, 5$ as a result, for the control set u , we have

$$\frac{\partial H}{\partial u^2} = 0, \quad \frac{\partial H}{\partial u} \Big|_{u=u^*} = Bu^* - \lambda_1 S^* + \lambda_5 S^* = 0,$$

and solve for u^* we will get

$$u^* = \frac{\lambda_1 S^* - \lambda_5 S^*}{B} \quad (25)$$

Using an appropriate variation argument and taking the bounds into consideration, the optimal control techniques are now stated.

$$u^* = \min \left\{ u_{\max}, \max \left(0, \frac{\lambda_1 S^* - \lambda_5 S^*}{B} \right) \right\} \quad (26)$$

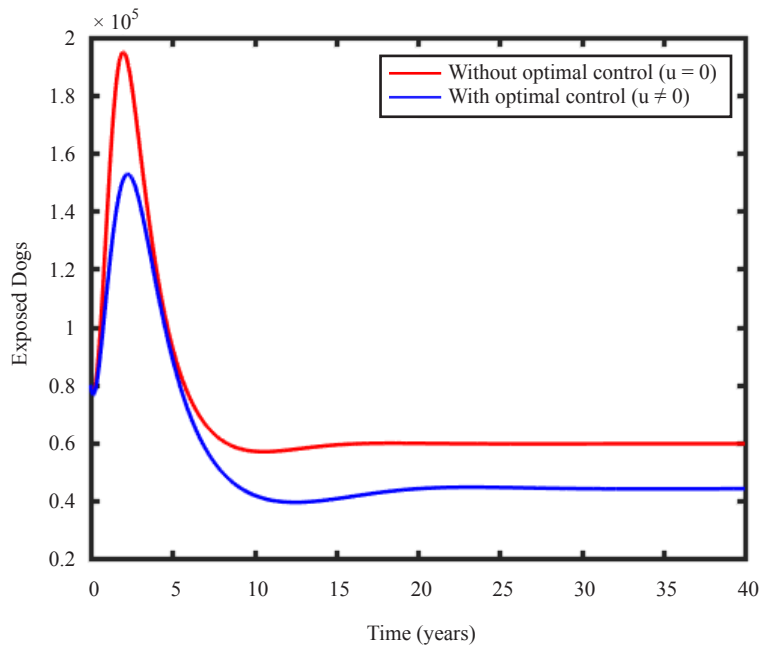


Figure 6. The function of Exposed individuals with and without control.

Figure 6 Compares the peaks of infected (Prodromal stage) dogs with optimal control (blue color curve) with those without control (red color curve), demonstrating that with the best control, there are fewer infected (Prodromal stage) dogs than there are without control. Moreover, figure 7. The blue color curve represents infected (Furious stage) dogs with optimal control, while the red color curve represents those without optimal control. The number of infected (Furious

stage) dogs is less than it would be without optimal control. Additionally, more dogs have been exposed due to the lack of optimal control. Observe Figure 8. In this, exposed dogs peak with control are fewer than those without control (blue color curve vs. red color curve).

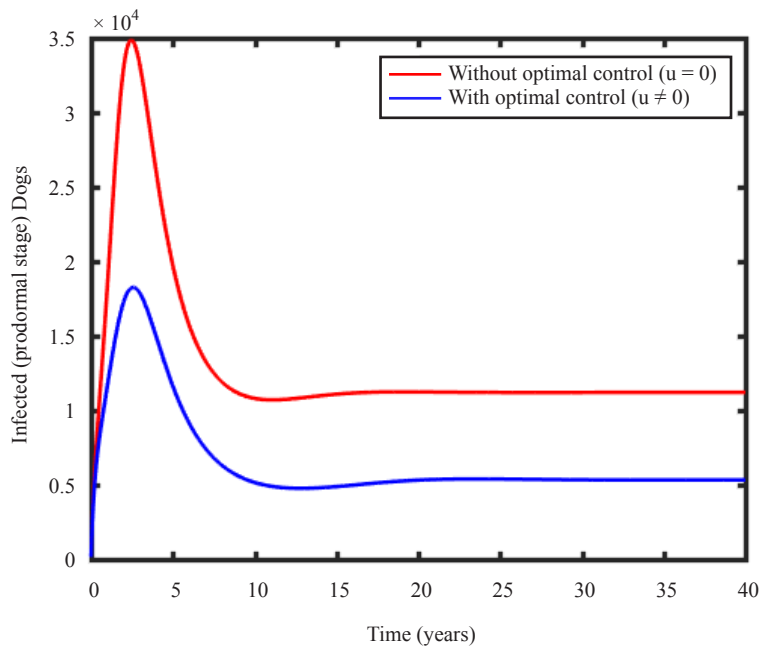


Figure 7. The function of Infected (Prodromal Stage) individuals with and without control.

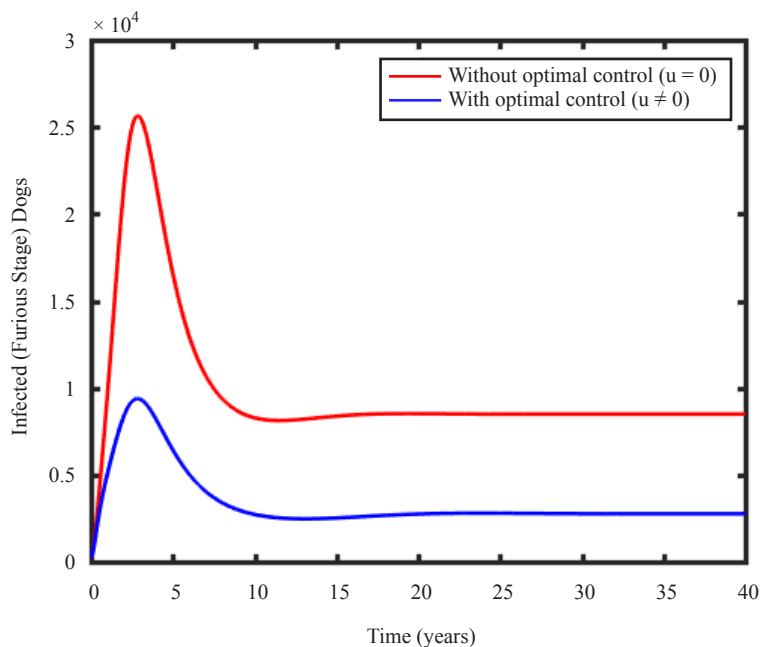


Figure 8. The function of Infected (Furious Stage) individuals with and without control.

7. Conclusion

In this paper, we have developed a deterministic compartmental mathematical model for the dynamics of rabies transmission. Traditional rabies is public in the dog population, the model was planned to show rabies transmission among dogs. In the model, vaccinations were applied to the susceptible dogs only. Vaccinating the exposed dogs is not practical because it is very difficult to identify the exposed dogs to be vaccinated. The basic properties of the epidemic models in terms of the boundedness and positivity of solutions are investigated for our model and we establish that the model is positive for all positive values of initial conditions. We conduct the equilibrium analysis, and stability analysis and derive the reproduction numbers. We establish that the disease-free equilibrium point is locally and globally asymptotically stable. The study also displays the model's sensitivity and optimal control analyses. The numerical simulations of the basic model are performed by varying the annual birth rate, vaccination, and culling rate. It is observed that increasing the vaccination and culling rate of dogs has a significant impact on the rate of spread of rabies transmission.

Data availability

The data used to support the findings of this manuscript are available from the corresponding author upon request.

Conflict of interest

The authors declare no competing financial interest.

References

- [1] World Health Organization (WHO). Rabies Fact Sheet. 2023. Available from: <https://www.who.int/news-room/fact-sheets/detail/rabies> [Accessed 21 May 2019].
- [2] Mayo Clinic. Rabies-symptoms and causes. 2016. Available from: <https://www.mayoclinic.org/diseases-conditions/rabies/symptoms-causes/syc-20351821>.
- [3] Zhang J, Jin Z, Sun G-Q, Zhou T, Ruan S. Analysis of rabies in China: Transmission dynamics and control. *PLoS One*. 2011; 6(7): 1-9.
- [4] Rabies. World Health Organization. 2023. Available from: <https://www.who.int/news-room/fact-sheets/detail/rabies>.
- [5] Addo KM. *An SEIR mathematical model for dog rabies. Case study: Bongo District, Ghana*. MSc. Dissertation Kwame Nkrumah University of Science and Technology; 2012. Available from: <http://dspace.knust.edu.gh:8080/jspui/handle/123456789/4100>.
- [6] Anderson RM. The kermack-mckendrick epidemic threshold theorem. *Bulletin of Mathematical Biology*. 1991; 53(1-2): 3-32. Available from: [https://doi.org/10.1016/S0092-8240\(05\)80039-4](https://doi.org/10.1016/S0092-8240(05)80039-4).
- [7] Keller JP, Gerardo-Giorda L, Veneziani A. Numerical simulation of a susceptible-exposed-infectious space-continuous model for the spread of rabies in raccoons across a realistic landscape. *Journal of Biological Dynamics*. 2013; 7(1): 31-46. Available from: <https://doi.org/10.1080/17513758.2012.742578>.
- [8] Hou Q, Jin Z, Ruan S. Dynamics of rabies epidemics and the impact of control efforts in Guangdong province, China. *Journal of Theoretical Biology*. 2012; 300: 39-47. Available from: <https://doi.org/10.1016/j.jtbi.2012.01.006>.
- [9] Pontragin LS, Gamkrelize RV, Boltyanskii VG, Mishchenko EF. *The Mathematical Theory of Optimal Processes*. Wiley; 1962.
- [10] Dejene D, Koya PR. Population dynamics of dogs subjected to rabies disease. *IOSR Journal of Mathematics (IOSR-JM)*. 2016; 12(3): 2319-2765. Available from: <https://doi.org/10.9790/5728-120304110120>.
- [11] Kadaleka S. *Assessing the effects of nutrition and treatment in cholera dynamics: The case of Malawi*. M. Sc. Dissertation, University of Der es Salaam; 2011.
- [12] Lakshmikantham V, Leela S, Kaul S. Comparison principle for impulsive differential equations with variable times and stability theory. *Nonlinear Analysis. Theory, Methods & Applications*. 1994; 22(4): 499-503.

- [13] Akalu A, Demsis D, Tadele A, Abayneh E. Mathematical modeling for COVID-19 transmission dynamics and the impact of prevention strategies: A case of Ethiopia. *International Journal of Mathematical Sciences and Computing (IJMSC)*. 2021; 7(4): 2310-9033.
- [14] Demsis DH, Tesfaye W, Rao Koya P. Modeling the transmission and dynamics of COVID-19 using self-protection and isolation as control measures. *Mathematical Modelling and Applications*. 2020; 5(3): 191-201.
- [15] Iggidr A, Mbang J, Sallet G, Tewa JJ. Multi-compartment models. *Discrete and Continuous Dynamical Systems-Series S*. 2007; 2007: 506-519. Available from: <https://doi.org/10.3934/proc.2007.2007.506>.
- [16] Stephen E, Nkuba NA. Mathematical model for the dynamics of cholera with control measures. *Applied and Computational Mathematics*. 2015; 4(2): 53-63.
- [17] Asamoah JKK, Oduro FT, Bonyah E, Seidu B. Modeling of rabies transmission dynamics using optimal control analysis. *Journal of Applied Mathematics*. 2017; 2017: 2451237. Available from: <https://doi.org/10.1155/2017/2451237>.
- [18] Demsis DH, Geremew KE, Koya PR. Effect of vaccination and culling on the dynamics of rabies transmission from stray dogs to domestic dogs. *Hindawi Journal Applied Mathematics*. 2022; 2022: 2769494. Available from: <https://doi.org/10.1155/2022/2769494>.
- [19] Ega TT, Luboobi LS, Kuznetsov D. Modeling the dynamics of rabies transmission with vaccination and stability analysis. *Applied and Computational Mathematics*. 2015; 4(6): 409-419.
- [20] Hethcote HW. The basic epidemiology models: Models expressions for r_0 , parameter estimation, and applications. *Mathematical Understanding of Infectious Disease Dynamics*. National University of Singapore, Singapore; 2008. p.1-61. Available from: https://doi.org/10.1142/9789812834836_0001.
- [21] Rachah A, Torres DFM. Mathematical modelling, simulation, and optimal control of the 2014 ebola outbreak in west Africa. *Nonlinear Dynamics in Epidemic Systems*. 2015; 2015: 842792. Available from: <https://doi.org/10.1155/2015/842792>.
- [22] Miller Neilan RL. *Optimal control applied to population and disease models*. Ph.D. diss., University of Tennessee; 2009. Available from: https://trace.tennessee.edu/utk_graddiss/74.
- [23] Pontryagin LS, Boltyanskii VG, Gamkrelize RV, Mishchenko EF. *The Mathematical Theory of Optimal Processes*. Wiley, New York; 1967.
- [24] Lenhart S, Workman J. *Optimal Control Applied to Biological Models*. 1st ed. Chapman Hall/CRC, New York; 2007. Available from: <https://doi.org/10.1201/9781420011418>.